

Testing the Validity of the Averaged  
Approximation for the IAsys<sup>§</sup>

D. A. Edwards\*

S. A. Jackson<sup>†</sup>

Technical Report No. 2002-3



DEPARTMENT  
OF  
MATHEMATICAL SCIENCES

University of Delaware  
Newark, Delaware

---

<sup>§</sup>This work was supported by the University of Delaware Research Foundation.

\*To whom correspondence should be addressed. Email address: [edwards@math.udel.edu](mailto:edwards@math.udel.edu). This work was supported by the University of Delaware Research Foundation.

<sup>†</sup>Current address: Federal Sector/Defense Group, Computer Sciences Corporation, Moorestown, NJ 08057-0902. Email address: [sethajackson@hotmail.com](mailto:sethajackson@hotmail.com)

# Testing the Validity of the Averaged Approximation for the IAsys<sup>§</sup>

D. A. EDWARDS\* AND S. A. JACKSON<sup>†</sup>

Department of Mathematical Sciences, University of Delaware, Newark, DE, 19716-2553

**Abstract**—One device used to measure rate constants is the IAsys, and the flow in such a device can be modeled as stagnation point flow. Due to the special nature of the flow, the effects of transport on a surface reaction near a stagnation point may be incorporated exactly as long as the initial concentration of bound state is uniform. However, if the bound state is nonuniform initially, a complicated integrodifferential equation arises for the evolution of the bound state. Such a form is inconvenient for data analysis. The averaged approximation replaces the nonuniform initial state with its average, thus simplifying the analysis. This approximation is correct to  $O(\text{Da})$  as the Damköhler number  $\text{Da} \rightarrow 0$ . A numerical simulation of the integrodifferential equation is performed which shows that the averaged approximation is useful even outside this regime.

**Keywords**—Surface-volume reactions, integrodifferential equations, numerical simulation, surface plasmon resonance, IAsys.

---

<sup>§</sup> This work was supported by the University of Delaware Research Foundation.

\* To whom correspondence should be addressed. E-mail address: [edwards@math.udel.edu](mailto:edwards@math.udel.edu). This work was supported by the University of Delaware Research Foundation.

<sup>†</sup> Current address: Federal Sector/Defense Group, Computer Sciences Corporation, Moorestown, NJ 08057-0902. E-mail address: [sethajackson@hotmail.com](mailto:sethajackson@hotmail.com).

## 1. INTRODUCTION

Many chemical reactions of interest in industrial and biological processes occur between one reactant (the *receptor*) which is attached to a surface and another (the *ligand*) that floats free in solution [1], [2]. These react on the receptor surface to form the *bound state*. In order to understand and hopefully control these reactions, one needs accurate measurements of the governing *rate constants* for the reaction. A key question is how to make real-time measurement of rate constants without disturbing the underlying systems.

The IAsys device is a resonant-mirror biosensor which allows such measurements [3]. It consists of a well containing the analyte solution, which is then agitated using a vibrostirrer. The reactant surface is on the well bottom (see figure 1). The flow near the surface can be approximated by stagnation point flow [4]. Reactant binding causes refractive changes in a polarized light beam which are then averaged over the reactant surface [3]. This data is then transferred to a regression program which predicts the rate constants using a mathematical model.

Unfortunately, until recently these models have treated only the case where the analyte and receptor are distributed uniformly along the reacting surface. The effect of the flow in the analyte was not considered, and hence the transport was essentially taken to be instantaneous. In this paper we discuss the complications that arise when nonuniformities are taken into account. There is an approximation that simplifies the complications substantially; it has been shown to be asymptotic for small transport effects. In this paper we demonstrate numerically that this *averaging approximation* is actually good for a wide parameter range.

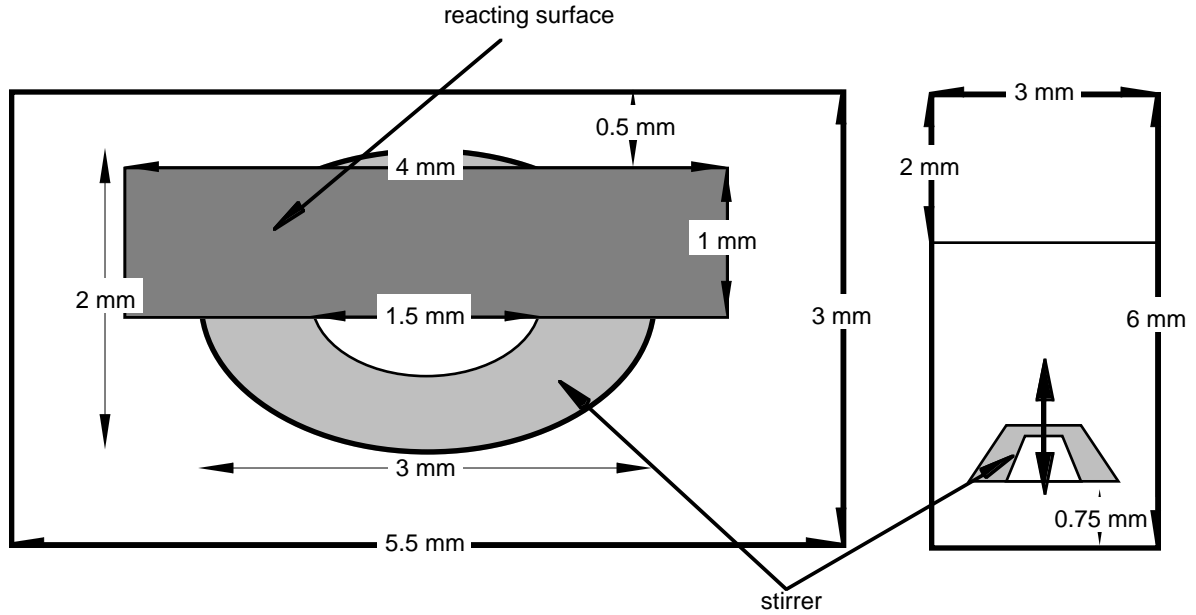


Figure 1. IAsys device, bottom and side view.

## 2. GOVERNING EQUATIONS

As mentioned above, the simplest case to consider is where transport effects are absent.

In this case, the reaction is governed by the simple (dimensionless) ODE

$$\frac{dB}{dt} = (1 - B) - KB, \quad (1)$$

where  $B$  is the proportion of the receptor sites bound and  $K$  is the *affinity constant*, which is a ratio of the rate constants [4]. In this case  $B$  is independent of position along the reacting surface and the averaging of the data does not affect the calculation of the rate constants.

By taking the well to be two-dimensional, one can construct a simple model for the IAsys system: that of flow about a stagnation point at the origin (see figure 2). In that case, it can be shown [4] that in the limit of large Peclet number (as is achieved in the

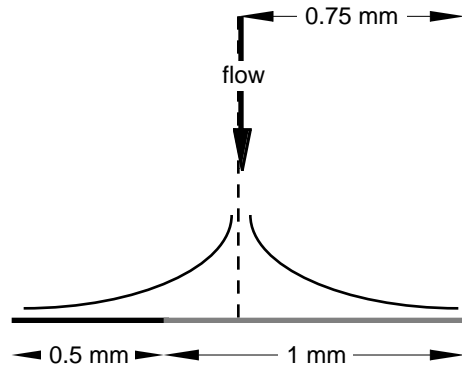


Figure 2. Stagnation-point idealization of IAsys device.

IAsys), the actual governing equation for  $B$  is as follows:

$$\frac{\partial B}{\partial t} = [1 - \text{Da}C(x)](1 - B) - KB, \quad B(x, 0) = B_i(x), \quad (2a)$$

$$C(x) = \frac{3^{1/3}}{2F^{1/3}\Gamma(2/3)} \int_0^x \frac{1}{(x^{3/2} - \xi^{3/2})^{2/3}} \frac{\partial B}{\partial t}(\xi, t) d\xi, \quad (2b)$$

$$\text{Da} = \frac{\tilde{k}_{\text{on}} R_T \nu^{1/6} H^{1/2}}{V^{1/2} \tilde{D}^{2/3}} = \frac{\text{reaction rate}}{\text{diffusion rate in unstirred layer}}.$$

Here  $x$  is distance from the stagnation point and  $C$  represents the deviation of the analyte concentration from the uniform value 1 implicit in equation (1). Also  $F \approx 0.616$  is a constant arising from the relevant Falkner-Skan equation for the viscous boundary layer near the sensor surface. Note from (2b) that as expected, the analyte depleted at  $x$  is an integral of the differential changes upstream ( $0 < \xi < x$ , as the problem is symmetric).

Here  $\text{Da}$  is the *Damköhler number*, which measures the strength of transport effects. It can range over several orders of magnitude (in particular, in [4] Edwards calculates a range of  $4.62 \times 10^{-7} \leq \text{Da} \leq 4.48 \times 10^4$ ), but typically the values are small, on the order of  $10^{-1}$  [4]. The “unstirred layer” refers to the boundary layer near the surface of width  $\text{Pe}^{-1/3}$  where diffusion and convection balance. In the definition of  $\text{Da}$ ,  $\tilde{k}_{\text{on}}$  is the association

(“on”) constant,  $R_T$  is the total number of sites available for binding,  $\nu$  is the viscosity of the solution,  $H$  and  $V$  are the characteristic height and velocity of the vibrostirrer, and  $\tilde{D}$  is the diffusion coefficient.

Due to the nature of the flow, the integral in (2b) is quite unusual. Essentially, the  $(x^{3/2} - \xi^{3/2})^{-2/3}$  term behaves like a weighted  $\delta$ -function. Thus, if  $\partial B/\partial t$  is uniform in  $x$ , the integral is *independent* of  $x$ . This implies that  $C$  is uniform, which forms a consistent system independent of  $x$ . Of course, for such a solution to satisfy (2), the initial condition  $B_i$  must also be independent of  $x$ . But if such a condition is satisfied, the solution  $B$  of (2) may be written as the solution of this equation [4], which is uniform in  $x$ :

$$\frac{dB}{dt} = [(1 - B) - KB](1 - p), \quad p = \frac{\text{Da}(1 - B)C_1}{1 + \text{Da}(1 - B)C_1}, \quad C_1 = \frac{\Gamma(1/3)}{3^{2/3}F^{1/3}}. \quad (3)$$

Equations in the general form of (3) have been seen in previous works [5]–[8], and are dubbed *effective rate constant* (ERC) equations. However, we note that in contrast to those works, equation (3) is *exact*. In [5]–[8], the ERC equation is an *asymptotic* solution of the full system analogous to (2). The ERC could be shown to be effective to  $O(\text{Da}^2)$  [5], though the error at that order is quite small [7], and the expression also seems to provide acceptable results *outside* its range of validity (*i.e.*, when  $\text{Da} = O(1)$ ) [8].

Since  $B$  is independent of  $x$ , (3) is in a form compatible with the averaged data stream. In a dissociation experiment,  $p$  is the probability that an analyte molecule dissociating from the surface will rebind further downstream [7], and here the interpretation is similar. Essentially,  $p$  is the probability that an analyte molecule will be unavailable for binding due to inefficient transport.

Therefore, not only is (3) a more useful form for analysis than (2), it also yields insightful physical interpretations. However, at this stage it has been determined to be useful only when  $B_i$  is independent of  $x$ . We now wish to extend this result by using

the *averaged approximation*. In cases where  $B_i$  depends on  $x$ , we replace the complicated system (2) with (3) by using the *average* of  $B_i$  as the initial condition for (3). We note that in the limit that  $\text{Da} \rightarrow 0$ , the nonlinearity in (2a) is  $O(\text{Da})$ , and hence the error inherent in the averaged approximation should be  $O(\text{Da})$  as  $\text{Da} \rightarrow 0$ .

### 3. NUMERICAL SIMULATIONS

We now present the results of a systematic series of simulations where solutions of (2) and (3) are compared to determine the efficacy of (3) when  $B_i$  depends on  $x$ . The algorithm used is quite similar to that in [8], which considered surface-volume reaction for a different flow. In particular, for (3) a standard explicit Euler scheme was used. Indexing space by time by  $n$ , a schematic version of the algorithm is shown below:

$$\frac{\partial B_{n+1}}{\partial t} = (1 - B_n - KB_n)(1 - p_n), \quad p_n = \frac{\text{Da}(1 - B_n)C_1}{1 + \text{Da}(1 - B_n)C_1}. \quad (4)$$

The algorithm for (2) is more subtle, reflecting the increased complexity of the problem. First, we note that due to the form of the convolution integral in (2b), the value of  $C(x, t)$  (and hence  $B(x, t)$ ) depends only on those values of  $B(\xi, t)$  for  $\xi \leq x$ . Therefore, by solving first at  $x = 0$  and working downstream for each time step, we may use *updated* values of  $\partial B/\partial t(\xi, t)$  at each grid point. Indexing space by  $j$ , a schematic version of the algorithm is shown below:

$$C_{j,n+1} = \frac{3^{1/3}}{2F^{1/3}\Gamma(2/3)} \int_0^{x_j} \frac{\partial B}{\partial t}(\xi, t_{n+1}) \frac{d\xi}{(x_j^{3/2} - \xi^{3/2})^{2/3}}. \quad (5a)$$

However, the scheme is not fully implicit; for the discretization of  $B$  in (2a), the value from the previous time step was used:

$$\frac{\partial B_{j,n+1}}{\partial t} = (1 - \text{Da}C_{j,n+1})(1 - B_{j,n}) - KB_{j,n}. \quad (5b)$$

This choice, though it makes the method only semi-implicit, rather than fully implicit, forces (5b) to reduce to (4) when  $Da = 0$ , thus ensuring consistency in the results.

Not only does the kernel of the integral behave like a  $\delta$ -function, but it also contains a singularity at  $\xi = x_j$  that cannot be computed directly. Because the integrand contains an unknown, we use the simplest possible method of removing the singularity: we subtract it from the integrand and computed it directly. Schematically, the algorithm replacing (5a) is as follows:

$$C_{j,n+1} = \frac{3^{1/3}}{2F^{1/3}\Gamma(2/3)} \times \left\{ \int_0^{x_j} \left[ \frac{\partial B}{\partial t}(\xi, t_{n+1}) - \frac{\partial B_{j,n+1}}{\partial t} \right] \frac{d\xi}{(x_j^{3/2} - \xi^{3/2})^{2/3}} + \frac{4\pi}{3\sqrt{3}} \frac{\partial B_{j,n+1}}{\partial t} \right\}. \quad (6)$$

Note that the term we subtract off depends on  $x_j$  only through  $\partial B_{j,n+1}/\partial t$ . This is consistent with the kernel behaving like a  $\delta$ -function. Since the bracketed quantity in the integrand of (6) is zero at  $\xi = x_j$ , the integrand is no longer singular, so the numerical integration can be performed using the Trapezoidal Rule.

In the IAsys, the data is averaged over the interval  $[-1/3, 1]$ . Since the problem is symmetric, this average can be converted to a weighted integral over the range  $[0, 1]$  [4]:

$$\bar{B} = \frac{3}{4} \left[ 2 \int_0^{1/3} B(x, t) dx + \int_{1/3}^1 B(x, t) dx \right]. \quad (7)$$

Therefore, once the solution was obtained, it was averaged using the Trapezoidal Rule on (7), with the *averaging transition value*  $1/3$  replaced by the closest grid point to  $1/3$ . (This error can be considered part of the discretization error.) Not only does this averaging simulate the actual data from the instrument, but also it smoothes any errors due to the singular nature of the kernel. The simulation ran until one of the derivatives in either (2) or (3) was less than a tolerance based on  $\Delta t$ .



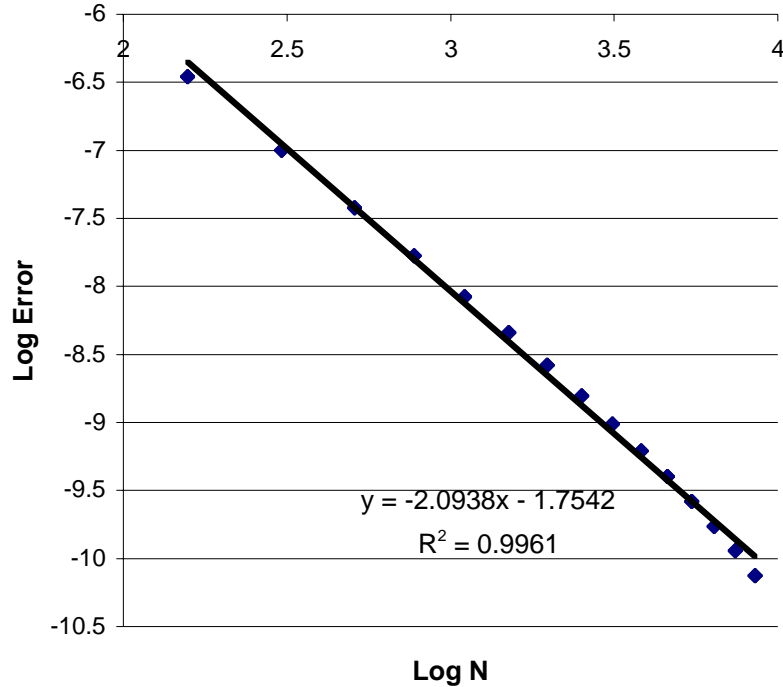


Figure 3. Error of discretized solution. The error plotted is the largest difference between the solution with  $N$  grid points and the solution with 81 grid points for a complete run with  $Da = 0.45$ ,  $K = 1$ ,  $B_i = 1 - x^2$ .

To test for accuracy, we performed several experiments with differing values of  $\Delta x$ , using the most refined solution as the baseline. The results are shown in Fig. 3. Since we were testing for accuracy, we chose  $B_i(x) = 0$ . To eliminate errors associated with approximating the averaging transition value, we chose only those  $N$  divisible by three. Since  $B_i$  does not have any singularities in the interval, neither will  $C$  (only the kernel does). Thus, the error is the standard trapezoidal error  $(\Delta x)^2$ . Therefore, we always set our time step equal to  $(\Delta x)^2$  to balance time and space errors.

To compare the accuracy of the averaged approximation, we graphed the error between the numerical solutions of (2) and (3) throughout an experiment. The results are shown in Fig. 4. As one can see, the error is quite small even though we are using an averaged initial condition.

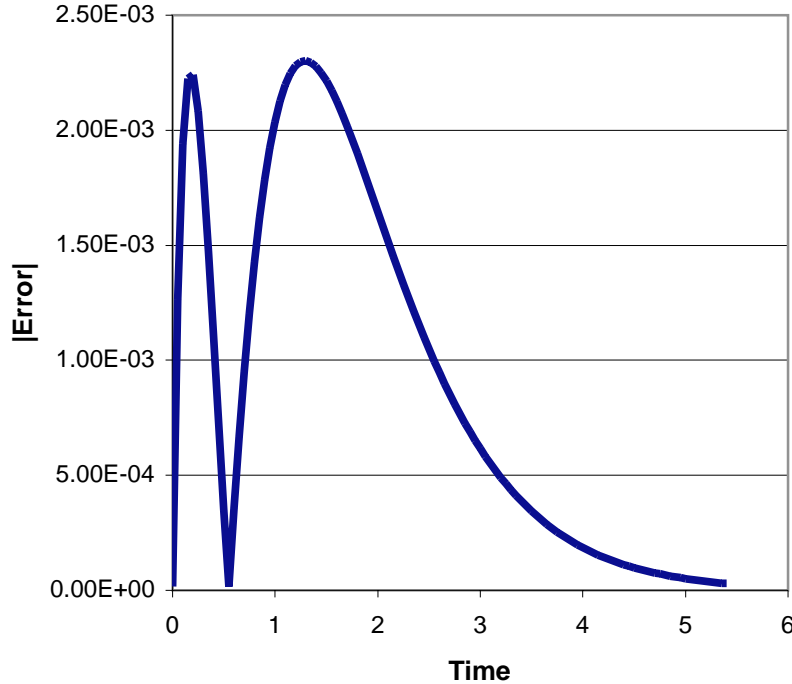


Figure 4. Error between averaged approximation and full numerical solution *vs.*  $t$  for a complete run with  $Da = 0.45$ ,  $K = 1$ ,  $B_i = 1 - x^2$ .

Lastly, we tested the main hypothesis: whether (3) can be used effectively with averaged initial conditions. An experiment was designed with  $\Delta x = 0.01$ , which corresponds to a discretization error of  $10^{-4}$ . The results are shown in Fig. 5. Note that for small  $Da$ , the error grows like  $Da$ , as predicted. Then as  $Da$  increases, the error remains small, eventually asymptoting to a maximum value as  $Da \rightarrow \infty$ . This is because as  $Da \rightarrow \infty$ ,  $p \rightarrow 1$  and we eventually reach a case where the transport is so slow that the downstream sites are starved for analyte. However, this asymptote is still small (corresponding to roughly a 2% error), and thus we see that the averaged approximation provides a good estimate to the true solution even when  $Da$  is not small, especially when one considers that there will be noise in any laboratory experiment.

#### 4. CONCLUSIONS

In order to obtain accurate rate constants using any device, one must have simple,

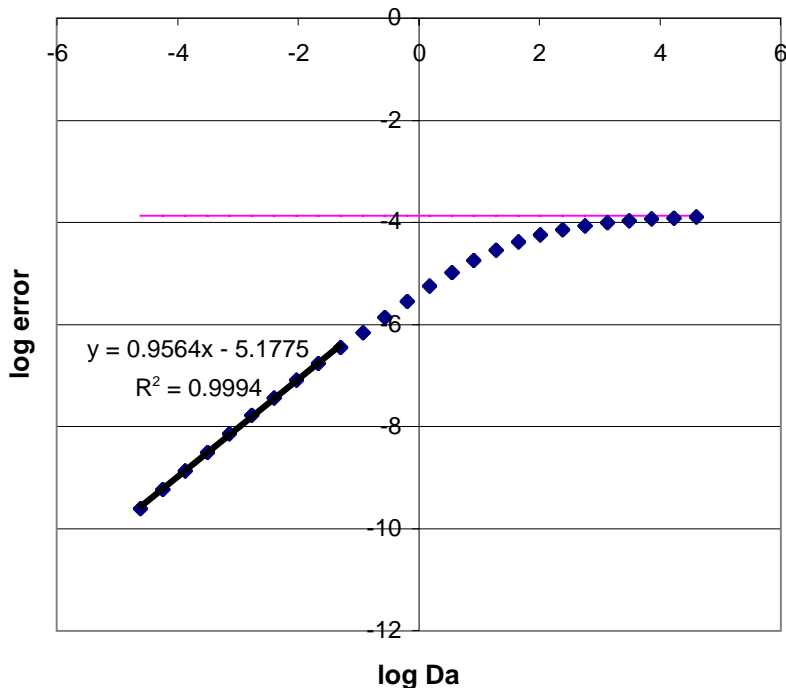


Figure 5. Error between averaged approximation and full numerical solution *vs.*  $Da$  for runs with  $K = 1$ ,  $N = 100$ ,  $B_i = 1 - x^2$ .

effective models for surface-volume reactions including transport. Through  $Da$ , transport slows the reaction from the well-mixed case. Thus, experimentalists try to adjust laboratory parameters to minimize the effects of transport.

The IAsys achieves this through the use of the vibrostirrer, which can generate high flow rates (nearly 40 cm/s) [4]. However, the finite volume of the well may introduce depletion effects (which we have ignored here) if there is not a large amount of analyte in solution. In contrast, the BIAcore, a competing surface plasmon resonance (SPR) device [9], consists of a channel through which the analyte flows. Here the effects of transport are manifested in depletion along the length of the channel, since the analyte inflow concentration is maintained as a constant.

However, in both devices one can often obtain an experimentally valid case where transport must be considered. In order to perform regression analysis for the parameters, it is better to have a simpler model than (2) to which to fit the data. In the IAsys, by

assuming a stagnation point flow and a uniform initial bound state, transport effects can be treated exactly in a simple ODE. The beauty of this result spurs us to find a way to use it even when the bound state is not uniform initially, where the exact treatment is a complicated integrodifferential equation.

In order to verify the efficacy of the resulting averaged approximation, we must construct an efficient algorithm for solving the exact system (2). The form of the integral in (2b) both helps and hinders the analysis. The fact that the integral covers only upstream values allows us to make much of the time stepping implicit. However, the nature of the integrand forces us to subtract off a singularity when doing the calculation. The resulting integrals and averaging can be performed with the Trapezoidal Rule.

Using the comparison tests, we showed that the averaged approximation is correct to  $O(\text{Da})$  as  $\text{Da} \rightarrow 0$ . In addition, with the calculations shown in Fig. 5, we see that even when transport effects play a significant role and  $\text{Da}$  is not small, the averaged approximation still provides useful rate constant estimates. In our particular test case, the averaged approximation remained within 2% of the solution of the full system, a similar result to the same calculation with the BIAcore model [8]. Thus introducing nonuniformities into the initial condition  $B_i$  need not necessitate going to the full model (2) instead of the averaged approximation (3) to obtain accurate rate constant estimates.

## REFERENCES

1. P. Duverneuil and J. P. Couderc, Two-dimensional modeling of low-pressure chemical vapor deposition hot wall tubular reactors. 1. Hypotheses, methods, and first results, *J. Electrochem. Soc.* **139**, 296–304 (1992).
2. M. Raghavan, M. Y. Chen, L. N. Gastinel, and P. J. Bjorkman, Investigation of the interaction between the class I MHC-related Fc receptor and its immunoglobulin G ligand, *Immunity* **1**, 303–315 (1994).

3. P. E. Buckle, R. J. Davies, T. Kinning, D. Yeung, P. R. Edwards, D. Pollardknight, C. R. Lowe, The resonant mirror: A novel optical sensor for direct sensing of biomolecular interactions. 2. Applications, *Biosen. Bioelec.* **8**, 355–63 (1993).
4. D. A. Edwards, Surface reaction near a stagnation point, *Stud. Appl. Math.* **105**, 1–29 (2000).
5. D. A. Edwards, Estimating rate constants in a convection-diffusion system with a boundary reaction, *IMA J. Appl. Math.* **62**, 89–112 (1999).
6. D. A. Edwards, B. Goldstein, and D. S. Cohen, Transport effects on surface-volume biological reactions, *J. Math. Bio.* **39**, 533–561 (1999).
7. T. Mason, A. R. Pineda, C. Wofsy, and B. Goldstein, Effective rate models for the analysis of transport-dependent biosensor data, *Math. Biosci.* **159**, 123–144 (1999).
8. D. A. Edwards and S. A. Jackson, Testing the validity of the effective rate constant approximation for surface reaction with transport, *Appl. Math. Lett.* **15**, 547–552 (2002).
9. A. Szabo, L. Stolz, and R. Granzow, Surface plasmon resonance and its use in biomolecular interaction analysis (BIA), *Curr. Opin. Struct. Bio.* **5**, 699–705 (1995).